Journal of Chemical&Engineering Data

Open Access

This article is licensed under CC-BY 4.0

pubs.acs.org/jced

Article

Partition of Chlorogenic and Nicotinic Acids Using Eco-Friendly ATPSs Containing Ethyl Lactate at 298.15 K and 0.1 MPa

Pedro Velho,* Gonçalo Perestrelo,* and Eugénia A. Macedo*

Cite This: *J. Chem. Eng. Data* 2024, 69, 3075−3084

Read Online

ACCESS | Metrics & More | Article Recommendations | Supporting Information

ABSTRACT: Biowaste, particularly food waste, could provide an alternative and more sustainable source for biomolecules such as antioxidants, allowing delays in the final treatment steps of these residues (*e.g.*, fertilizer production and incineration) and even reduction of the amount of final waste. Furthermore, the application of green solvents such as ethyl lactate in aqueous two-phase systems (ATPSs) provides a biocompatible medium with high water content and promising scale-up potential. Nevertheless, a preliminary lab-scale evaluation of the extraction of each antioxidant using ATPSs is vital for the success of pilot-scale operations. In this work, partition studies were carried out for chlorogenic acid (ChloA) and nicotinic acid (NicoA) at 298.15 K and 0.1 MPa in the ATPSs {ethyl lactate (1) + NaKTartrate or Na_3Citrate or K_3Citrate (2) + water (3)}. The largest performance indicators of extraction for ChloA were obtained using Na_3Citrate, achieving a maximum partition coefficient (K) of 10 ± 1 and a maximum extraction efficiency (E) of 90.4 ± 0.9% in the longest tie-line [tie-line length (TLL) = 69.68%], while for NicoA, the most successful extraction, with K = 6.5 ± 0.5 and E = 86.8 ± 0.8%, was observed for the ATPS with K_3Citrate (TLL = 77.66%). The obtained partition coefficients and extraction efficiencies were checked by calculating the mass losses in quantification (L_s), which were lower than 4%, validating the analytical method and allowing to conclude that the studied ATPSs could provide an efficient and eco-friendly extraction medium for NicoA and ChloA.

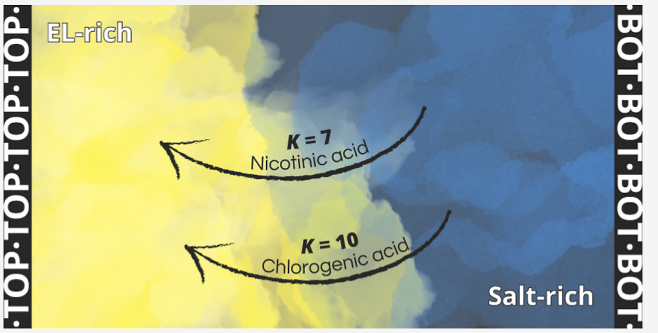

1. INTRODUCTION

Chlorogenic acid (ChloA) and nicotinic acid (NicoA) are strong antioxidants present in food waste which could be extracted without decreasing the efficiency of agricultural fertilizers or the yield of incineration plants (common destinies of this feedstock[1]), boosting a better valorization of biowaste and forwarding a more circular economy.

Due to the antioxidant and antimicrobial activity of ChloA, it has an extensive application in the food industry, namely, as an emulsifier, colorant, and preservative.[2] Furthermore, ChloA is also used in pharmaceutical products given its anti-inflammatory and antiobesity properties.[3,4] Concerning NicoA, its commercial use is significantly lower, mostly residing in medicines to control the unbalance of blood lipids (antidyslipidemic property).[5]

Regarding their natural occurrence in food, ChloA is commonly found in apples, potatoes, and green coffee,[6] while NicoA is typically present in chestnuts, peaches, and cherries,[7] so using residues such as peels and seeds as raw materials for the obtainance of these polyphenols would avoid diverting high-nutrition food crops to industrial uses. Nevertheless, the development of more sustainable processes and biocompatible extraction media, which often require years of continuous improvement, is crucial for an efficient and profitable recovery of antioxidants.

Aqueous two-phase systems (ATPSs) constitute a liquid−liquid extraction technique with low environmental impact which has been greatly applied in the recovery of biomolecules such as proteins,[8−10] vitamins,[11−13] and antioxidants,[14−17] generally providing extraction media with low interfacial tension and toxicity, high biocompatibility, and scale-up potential.[18] Therefore, these systems could provide a promising alternative for the extraction of polyphenols without damaging their bioactivity.[12]

However, not all ATPSs are suitable for the extraction of such labile species, so green solvents such as ethyl lactate, which couple large solvent power with high nontoxicity,[19,20] may be used to increment the biocompatibility of ATPSs. Moreover, this solvent can be synthesized by the fermentation of biowaste and is considered a promising alternative to petroleum derivatives, presenting a wide range of commercial applications in industries such as food, perfumes, and coatings.[21]

Received: April 12, 2024
Revised: May 24, 2024
Accepted: June 3, 2024
Published: June 20, 2024

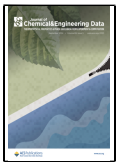

Downloaded via UNIVERSIDADE DO PORTO 01100 on November 14, 2024 at 14:39:39 (UTC).
See https://pubs.acs.org/sharingguidelines for options on how to legitimately share published articles.

ACS Publications

© 2024 The Authors. Published by American Chemical Society

https://doi.org/10.1021/acs.jced.4c00197
J. Chem. Eng. Data 2024, 69, 3075−3084

Table 1. List of Chemicals, with Their Respective Chemical Formula, Supplier, Purity, CAS Number, and Abbreviation

chemical	supplier	purity / %[a]	CAS	abbreviation
acetic acid ($C_2H_4O_2$)	Merck	>99.8	64-19-7	AA
chlorogenic acid ($C_{16}H_{18}O_9$)	Apollo Scientific	>98.0	327-979	ChloA
ethanol (C_2H_6O)	Sigma-Aldrich	>99.0	64-17-5	EtOH
(−)-ethyl L-lactate ($C_5H_{10}O_3$)	Sigma-Aldrich	>98.0	97-64-3	EL
nicotinic acid ($C_6H_5NO_2$)	Sigma-Aldrich	>99.0	59-67-6	NicoA
purified water (H_2O)	VWR chemicals	[b]	7732-18-5	W
sodium hydroxide (NaOH)	Merck	>99.0	1310-73-2	NaOH
sodium potassium tartrate tetrahydrate ($C_4H_4NaKO_6{\cdot}4H_2O$)	Sigma-Aldrich	>99.0	6381-59-5	NaKTartrate
tripotassium citrate monohydrate ($C_6H_5K_3O_7{\cdot}H_2O$)	Sigma-Aldrich	>99.0	6100-05-6	K_3Citrate
trisodium citrate dehydrate ($C_6H_5Na_3O_7{\cdot}2H_2O$)	VWR chemicals	>99.0	6132-04-3	Na_3Citrate

[a]Provided by the supplier in mass percentage. [b]The electrical conductivity (k) of pure water was found to be 5×10^{-6} S·m^{-1}.

To reduce experimentation and to help find the most promising pairs of ATPS and biomolecules, computational chemistry can be used. It optimizes the chemical structure of solutes in the solvent media, allowing one to have a rough estimate of solute migration. In particular, density functional theory (DFT) is a computational quantum mechanical modeling methodology with wide application in academia due to its favorable compromise between accuracy and computational cost.[22] Nevertheless, it has a practical limit of 500 atoms and is known to take long computational times when applied to large systems.[23]

In this work, partition assays were conducted for ChloA and NicoA at 298.15 K and 0.1 MPa in the ATPSs {ethyl lactate (1) + NaKTartrate or Na_3Citrate or K_3Citrate (2) + water (3)} as a decisive preliminary study for the extraction of these polyphenols from food waste. Moreover, computational chemistry was used to ease the interpretation of the results.

2. EXPERIMENTAL SECTION

2.1. Materials. The chemicals used in this work, as well as their respective supplying companies, purities, Chemical Abstracts Service (CAS) numbers, and abbreviations, can be found in Table 1. These compounds were used as provided by the suppliers, for which no additional purification steps were conducted. The chemical structures of ChloA and NicoA are shown in Figure S1 in the Supporting Information.

2.2. Equipment. To quantify mass (m), an Adam Equipment AAA 250L balance, with a standard measurement uncertainty of 10^{-4} g, was used, while pH was measured with a VWR pH 1100L device, with standard measurement uncertainties of 0.01 in pH and 0.1 K in temperature (T). To confirm the water content of antioxidants and organic salts, a Mettler Toledo C20 Coulometric Karl Fisher titrator, with a standard measurement uncertainty of 5 ppm, was applied, with hydrate water being accounted for during solution preparation. Moreover, the electrical conductivity (k) of pure water was checked with a Hanna EDGE EC conductivity meter, coupled with a platinum conductivity cell HI763100, with a relative measurement uncertainty of 0.01. Concerning ultraviolet−visible (UV−vis) absorbance, a ThermoScientific Varioskan Flash UV−vis spectrophotometer, with a standard measurement uncertainty of 10^{-4}, was applied, and liquid density (ρ) was quantified with an Anton Paar DSA-4500 M oscillating densimeter, with standard measurement uncertainties of 3×10^{-5} g·cm^{-3} and 0.01 K. To control temperature, a Julabo F12 water bath with a standard measurement uncertainty of 0.1 K was used, with the temperature being rechecked with a manual glass thermometer (with a standard measurement uncertainty of 0.01 K). The densimeter and pH meter were calibrated according to their manuals prior to experimentation.

2.2.1. Effect of pH on the Mean Electrical Charge. The pH of the extractive media is known to affect the mean electrical charge (q) of biomolecules,[12,15] which significantly impacts solute partition due to changes in hydrophobicity and conductivity. Therefore, it is vital to properly characterize the target antioxidants by calculating the relative abundance (or fraction, x_A) of their feasible oxidative states, following eq 1.[19] This equation is a generalization of the relations expressed by the negative base-10 logarithms of the acid dissociation constants (pK_a) of each antioxidant, which are translated by eq 2.

$$x_{A^{q_0-i+1}} = \frac{[A^{q_0-i+1}]}{[A^{q_0-1}]} \Bigg/ \left(\frac{[A^{q_0}]}{[A^{q_0-1}]} + 1 + \sum_{j=2}^{i_{max}} \left[\prod_{k=2}^{j} \frac{[A^{q_0-k}]}{[A^{q_0-(k-1)}]} \right] \right) \quad (1)$$

$$\frac{[A^{q_0-i+1}]}{[A^{q_0-i}]} = 10^{pH_{phase}-pK_a^i} \quad (2)$$

where q_0 is the electrical charge of the antioxidant A at pH = 0, i is the number of donated protons, i_{max} is the maximum number of protons, $x_{Aq0-i+1}$ is the fraction of species with electrical charge equal to $(q_0 - i + 1)$ e, pH_{phase} is the pH of the extractive medium, and $[A^{q_0-i+1}]$ and $[A^{q_0-i}]$ are the mole concentrations of the oxidative species with electrical charges equal to $(q_0 - i + 1)$ e and $(q_0 - i)$ e, respectively. e refers to the elementary charge (1.602×10^{-19} C).

After having found the relative abundance of each oxidative state, the calculation of the mean electrical charge (q) is performed using a weighted arithmetic mean, as eq 3 shows.[19]

$$q = \sum_{i=1}^{i_{max}} [x_{A^{q_0-i+1}} \cdot (q_0 - i + 1)] + [1 - \sum_{i=1}^{i_{max}} (x_{A^{q_0-i+1}})] \cdot (q_0 - i_{max}) \quad (3)$$

2.2.2. Effect of pH on the UV−Vis Absorbance Spectrum. The existence of different oxidative states of each antioxidant depending on pH may lead to different UV−vis absorbance spectra due to changes in the chemical conformation and structure. Hence, to decrease experimental error during quantification by UV−vis spectroscopy, aqueous solutions of the target antioxidants, ChloA and NicoA, were prepared at approximately 1.44×10^{-4} and 3.68×10^{-4} g g^{-1}, respectively. Afterward, their pH values were adjusted by adding droplets of

https://doi.org/10.1021/acs.jced.4c00197
J. Chem. Eng. Data 2024, 69, 3075−3084

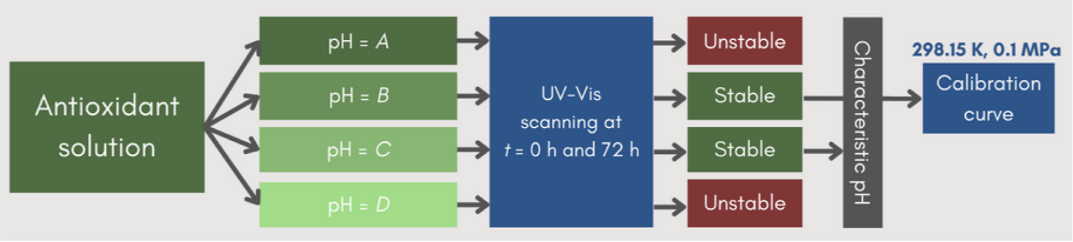

Figure 1. Procedure to assess the effect of pH on the UV−vis absorbance spectra of antioxidants.

0.5 M aqueous solutions of sodium hydroxide (NaOH) or acetic acid (CH_3COOH) to conditions in which the mean electrical charges were close to integer numbers to characterize a single oxidative state and assess the effect of pH on its UV−vis absorbance spectrum. Next, to evaluate the stability of the UV−vis spectra with time, an UV−vis absorbance measurement was conducted in the 200−600 nm range for all samples in the moment of preparation and after having settled for 3 days. To ease comparison and reduce the effect of dilution by the pH adjusters, the UV−vis absorbance spectra were normalized using eq 4, which is valid for minor differences in concentration.

$$A' = A \cdot \frac{C_{pH\approx 7}}{C_{pH=k}} \tag{4}$$

where A and A' are the measured and normalized UV−vis absorbances, respectively, $C_{pH\approx 7}$ is the reference concentration (chosen based on the characteristic pH of the studied ATPSs), and $C_{pH=k}$ is the concentration of the antioxidant solution at a defined pH.

Finally, calibration curves of UV−vis absorbance with antioxidant concentration were determined using triplicate measurements at pH ≈ 7, P = 0.1 MPa, and T = 298.15 K at the wavelength of local spectrum maxima by measuring the UV−vis absorbance of aqueous solutions with known antioxidant concentrations and adjusting the obtained data to a first-degree expression, as eq 5 shows.

$$A = \alpha C + \beta \tag{5}$$

where A is absorbance, α is the slope of the calibration curve (absorptivity), C is the antioxidant concentration (in g·mL^{-1}), and β is the y-intercept.

The overall procedure to assess the effect of pH on the UV−vis absorbance spectra is summarized in Figure 1. First, antioxidant solutions with a similar concentration were prepared at different pH values. Then, their UV−vis spectra were measured. Finally, if the spectra were stable after 3 days (and corresponded to the characteristic pH of any studied ATPS), an UV−vis calibration curve was determined.

2.2.3. Liquid−Liquid Equilibria Data. The liquid−liquid equilibria (LLE) data, *i.e.*, tie-line compositions, of the used ATPSs were found in previous works of the research group,[24,25] as Table 2 shows, and the respective phase equilibria diagrams can be found in Figure S2 in the Supporting Information.

2.2.4. Partition of Antioxidants. To assess solute partitioning in the studied ATPSs, two performance indicators of extraction were determined: the partition coefficients (K) and extraction efficiencies (E). The partition or distribution coefficients (K), calculated using eq 6, refer to the antioxidant concentration ratio between the two phases of the same tie-line. This performance indicator is calculated far from saturation and has been successfully predicted using thermodynamic modeling,[26,27] while estimating extraction efficiencies has been proven to be more difficult.

Table 2. Used Tie-Line Compositions for the ATPSs {Ethyl Lactate (1) + Sodium Potassium Tartrate[24] or Trisodium Citrate[25] or Tripotassium Citrate[25] (2) + Water (3)} at 298.15 K and 0.1 MPa.[ab]

	feed				separation		
tie-line	w_1 / %	w_2 / %	TLL / %	phase	w_1 / %	w_2 / %	pH
{Ethyl Lactate (1) + NaKTartrate (2) + Water (3)}[24]							
1	32.0	13.0	43.10	top	53.8	13.0	6.62
				bottom	13.7	20.0	6.61
2	34.3	13.3	52.13	top	59.0	13.3	6.71
				bottom	10.8	22.9	6.56
3	36.5	13.7	60.15	top	63.7	13.7	6.64
				bottom	8.2	25.5	6.56
4	38.5	13.9	64.59	top	66.2	13.9	6.65
				bottom	6.9	27.7	6.56
5	41.4	14.2	70.73	top	70.0	14.2	6.61
				bottom	5.4	30.5	6.56
{Ethyl Lactate (1) + Na_3Citrate (2) + Water (3)}[25]							
1	30.0	11.0	37.85	top	51.7	3.0	7.00
				bottom	16.0	15.7	6.98
2	32.0	11.4	48.18	top	57.5	2.0	6.98
				bottom	12.3	18.5	6.96
3	34.3	11.7	55.17	top	61.5	1.4	6.98
				bottom	9.8	20.7	6.97
4	36.5	12.1	61.17	top	65.0	1.0	7.00
				bottom	7.9	23.0	7.00
5	38.5	12.3	65.44	top	67.7	0.7	6.98
				bottom	6.8	24.7	6.97
6	40.6	12.6	69.68	top	70.1	0.5	6.98
				bottom	5.5	26.6	7.00
{Ethyl Lactate (1) + K_3Citrate (2) + Water (3)}							
1	35.5	12.6	45.91	top	57.9	3.9	7.21
				bottom	15.0	20.3	7.39
2	37.5	13.0	54.02	top	61.7	3.4	7.22
				bottom	11.5	23.2	7.41
3	39.2	13.5	62.96	top	67.4	2.1	7.19
				bottom	9.1	25.8	7.37
4	41.1	13.9	68.28	top	70.4	1.6	7.23
				bottom	7.5	28.2	7.41
5	43.0	14.3	73.92	top	73.6	1.1	7.12
				bottom	6.0	31.0	7.39
6	44.6	14.8	77.66	top	75.8	0.9	7.22
				bottom	5.2	33.1	7.43

[a] w_i stands for the mass percentage of species i. [b] The reported standard measurement uncertainties (u) are $u(T)$ = 0.1 K, $u(P)$ = 2 kPa, $u(w_i) = 10^{-1}$, and $u(\text{pH}) = 10^{-2}$.

https://doi.org/10.1021/acs.jced.4c00197
J. Chem. Eng. Data 2024, 69, 3075−3084

$$K_i = \frac{C_{T,i}}{C_{B,i}} \tag{6}$$

where i is the tie-line number and C_T and C_B are the calculated antioxidant concentrations in the top and bottom phases, respectively. These concentrations were determined using the previously obtained calibration curves (in g·mL^{-1}) and after the blanks had been subtracted from the measured UV−vis absorbances.

It must be noted that during partition studies, it is assumed that the presence of a solute (antioxidant) does not change the phase composition of the ATPSs. The antioxidant eventually migrates from one phase to another, but the relative composition between the top and bottom phases is assumed to be equal to the one determined in the absence of the target solute, as presented in Table 2.

On the other hand, the extraction efficiency or recovery (E), calculated following eq 7, refers to the percentage of antioxidant (in mass) which was isolated in the top phase of each tie-line. Nevertheless, this performance indicator is greatly affected by the location of the feed composition within the tie-line since it significantly affects the mass of the top phases. For this reason, extraction efficiencies are harder to predict by thermodynamic modeling and provide a less reliable comparison indicator than partition coefficients.

$$E_i = \frac{C_{T,i}V_{T,i}}{m_{SF,i}}\cdot 100 \tag{7}$$

where m_{SF} is the feed mass of antioxidant, C is the antioxidant concentration (in g·mL^{-1}), and V is the phase volume, which was calculated using eq 8. T refers to the top phase.

$$V_{f,i} = \frac{m_{f,i}}{\rho_{f,i}} \tag{8}$$

where f refers to the top (T) or bottom (B) phase, m is the phase mass, and ρ is the measured phase density.

As described above, mass (m), UV−vis absorbance (A), liquid density (ρ), and pH were measured for all phases, with mass losses in separation (L_m) being quantified using eq 9. Moreover, following previous works of the research group,[12,15] to validate the obtained performance indicators, the antioxidant losses in quantification (L_s) were calculated using eq 10. Determining the values of L_s allows comparison of the quantified amount of antioxidant with the added one in the feed of each tie-line.

$$L_{m,i} = \frac{(m_{T,i} + m_{B,i}) - m_{F,i}}{m_{F,i}}\cdot 100 \tag{9}$$

where m_F refers to the feed mass, m_T to the mass of the top phase, and m_B to the mass of the bottom phase.

$$L_{s,i} = \frac{m_{SQ,i} - m_{SF,i}}{m_{SF,i}}\cdot 100 \tag{10}$$

where m_{SF} and m_{SQ} are the feed and quantified masses of the antioxidant, respectively, with the latter being determined using eq 12.

$$m_{SQ,i} = C_{T,i}V_{T,i} + C_{B,i}V_{B,i} \tag{12}$$

where i is the number of tie-lines, C is the antioxidant concentration (in g·mL^{-1}), and V is the phase volume. Once again, T and B refer to the top and bottom phases, respectively.

3. RESULTS AND DISCUSSION

3.1. Effect of pH on the Mean Electrical Charge. The effect of the pH of the extraction media on the mean electrical charge (q) of ChloA and NicoA was studied using eq 3 and based on the pK_a values reported in literature for these antioxidants (ChloA: 3.50, 8.42, and 11.00;[28] NicoA: 4.95[29]). As Figure 2 illustrates, the mean electrical charge decreases with

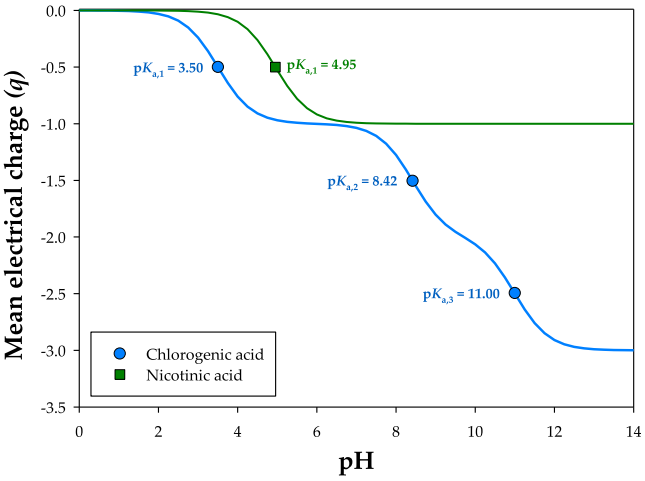

Figure 2. Calculated mean electrical charges (q) with pH for ChloA (with pK_a values of 3.50, 8.42, and 11.00[28]) and NicoA (with a pK_a value of 4.95[29]).

growing pH due to the sequential donation of protons (H^+), and NicoA always presents a less negative mean electrical charge than that of ChloA.

The mean electrical charge is known to affect the chemical conformation of the species, together with their polarity and hydrophobicity, for which it is an essential property for the assessment of solute migration. Moreover, at the characteristic pH of the studied ATPSs (pH ≈ 7), both antioxidants showed close to integer values of q (ChloA: q = −1.04 e; NicoA: q = −0.99 e), which are expected to foster the stability of the solution and ease quantification. The full data can be observed in Tables S1−S2 in the Supporting Information.

3.2. Effect of pH on the UV−Vis Absorbance Spectra. Following the determined mean electrical charges (q), aqueous solutions of the antioxidants (ChloA: ∼1.44 × 10^{-4} g·g^{-1}; NicoA: ∼2.49 × 10^{-4} g·g^{-1}) were prepared at pH values of interest to evaluate the effect of this property on the UV−vis absorbance spectra by adding droplets of 0.5 M aqueous solutions of sodium hydroxide (NaOH) or acetic acid (CH_3COOH). As Figure 3 shows, for ChloA, the UV−vis absorbance spectrum was notably affected by the pH of the medium, concerning both the intensity and the location of the relative maximum, which was found at 325 nm at pH = 7.21. For NicoA, only the intensity of the peaks varied, with higher pH values leading to smaller UV−vis absorbances. Moreover, the relative maximum for this antioxidant was found to be 264 nm at pH = 7.41.

To ensure that the determined UV−vis absorbance spectra shown in Figure 3 were stable up to the end of the experimental assays, which generally take approximately 24 h, as described in Section 2.2.4, the UV−vis absorbance spectra screenings of the prepared solutions were repeated after 3 days. Table 3, which summarizes the obtained conclusions, shows that at the characteristic pH of the studied ATPSs (pH ≈ 7), the obtained

https://doi.org/10.1021/acs.jced.4c00197
J. Chem. Eng. Data 2024, 69, 3075−3084

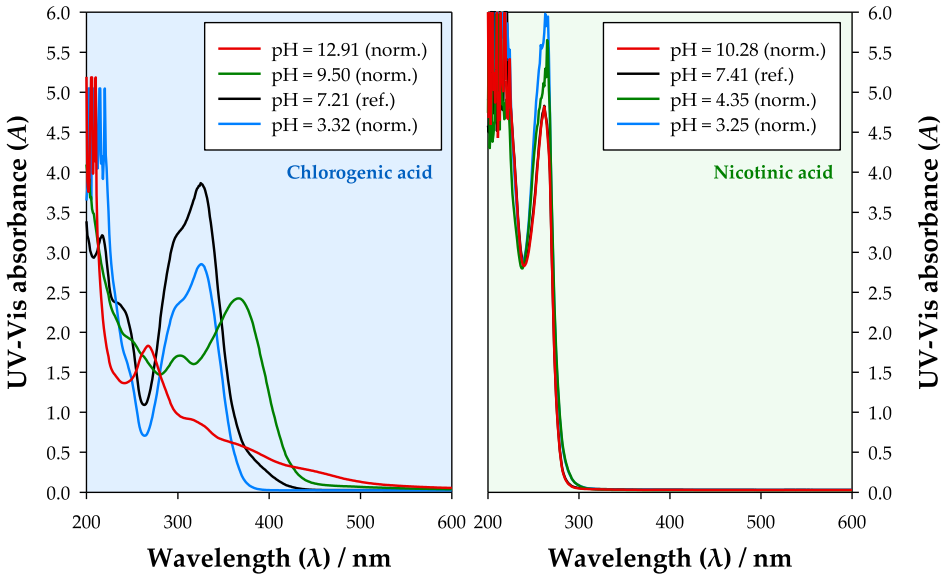

Figure 3. Effect of pH on the UV−vis absorbance spectra of ChloA (~1.44×10^{-4} g·mL^{-1}) (left) and NicoA (~2.49×10^{-4} g·mL^{-1}) (right). Some spectra were normalized using eq 4 to reduce the effect of dilution by pH adjustment.

Table 3. Stability Assessment of the UV−Vis Absorbance Spectra of ChloA and NicoA after 3 Days[a]

species	pH ≈ 3	pH ≈ 4	pH ≈ 7	pH ≈ 10	pH ≈ 13
ChloA	stable		stable	unstable	stable
NicoA	stable	stable	stable	stable	

[a]"Stable" refers to remarkably similar spectra, while "unstable" denotes a notable change in peak intensity and/or location.

UV−vis spectra of ChloA and NicoA were stable, allowing solute quantification in the partition assays by UV−vis spectroscopy. Hence, UV−vis calibration curves were determined at 325 and 264 nm for ChloA and NicoA, respectively.

3.3. Partition of Antioxidants. Once stirred for 6 h and settled overnight at 298.15 K and 0.1 MPa, phase separation in the ATPSs was notorious, for which the top and bottom phases were removed from the vials using syringes. Then, mass (m), liquid density (ρ), and pH of each phase were measured, and mass losses in phase separation (L_m) were calculated by using eq 9, as Table 4 shows.

As Table 4 shows, small losses in phase separation were observed in all ATPSs ($L_m < 1\%$), with the top phases presenting smaller values of liquid density (ρ). Moreover, a more preponderant difference in pH was observed between the phases of each tie-line compared to the one shown in Table 2, with the top phases exhibiting pH values significantly smaller than those of the bottom phases during the partition studies. This fact hints at a higher antioxidant concentration in the top phases, given the acidic character of ChloA and NicoA, which was confirmed after measuring the UV−vis absorbance and using the determined calibration curves, as Table 5 shows.

As Table 5 shows, the determined performance indicators were checked by calculating the mass losses in quantification (L_s), which were always lower than 4%, validating the analytical method. The most promising performance indicators of extraction for ChloA were obtained using trisodium citrate ($Na_3Citrate$), achieving a maximum partition coefficient (K) of 10 ± 1 and a maximum extraction efficiency (E) of $90.4 \pm 0.9\%$ in the longest tie-line (TLL = 69.68%). For NicoA, the most successful extraction, with $K = 6.5 \pm 0.5$ and $E = 86.8 \pm 0.8\%$, was observed in the longest tie-line (TLL = 77.66%) of the ATPS with tripotassium citrate ($K_3Citrate$). Furthermore, all obtained partition coefficients were significantly higher than unity, showing that the top phase had a higher affinity for the studied antioxidants than the bottom phase.

As Figure 4 shows, the natural logarithm of the partition coefficients presented a close to linear relationship with the tie-line length (TLL) in the studied ATPSs, with sodium-based salts favoring the migration of ChloA toward the top phases (EL-rich) and potassium-based ones backing increased concentrations of NicoA in these phases.

The obtained results were compared with others available in literature following the same methodology, and it was found that the maximum partition coefficients in each ATPS followed the order: resveratrol (41 ± 9)[15] > ChloA (8.0 ± 0.7) > NicoA (4.7 ± 0.3) > epicatechin (4.4 ± 0.2)[30] in NaKTartrate; resveratrol (19 ± 5)[15] > ChloA (10 ± 1) > epicatechin (5.44 ± 0.01)[19] > NicoA (3.55 ± 0.09)[12] in $Na_3Citrate$; and resveratrol (40 ± 6)[15] > epicatechin (24.86 ± 0.09)[12] > ChloA (9 ± 1) > NicoA (6.5 ± 0.5) in $K_3Citrate$.

To evaluate the effect of considering different units in antioxidant concentration (C), the partition coefficients (K) of the conducted liquid−liquid extractions were recalculated with concentrations on mass (w) and molar fraction (x), as Figures S3 and S4, respectively, show. It was found that partition coefficients based on concentrations in g·mL^{-1} and g·g^{-1} were very similar, with the latter presenting slightly higher values but preserving the relation between the systems. Furthermore, the ones based on molar fractions were found to be significantly larger, with partition coefficients even following a different order: NaKTartrate > $Na_3Citrate$ > $K_3Citrate$ for ChloA and NaKTartrate > $K_3Citrate$ > $Na_3Citrate$ for NicoA. Hence, to ensure a proper interpretation of this performance indicator and a correct representation using thermodynamic modeling, the units of concentration must always be taken into careful regard.

Given the similar mean electrical charges (q) found for ChloA ($q = -1.04$ e at pH = 7) and NicoA ($q = -0.99$ e at pH = 7), comparable partition coefficients would be expected for these antioxidants, but that was not the case, and ChloA presented significantly larger values of this performance indicator.

https://doi.org/10.1021/acs.jced.4c00197
J. Chem. Eng. Data 2024, 69, 3075−3084

Table 4. Experimental Mass (m), Phase Mass Loss (L_m), Liquid Density (ρ), and pH of Each Phase for the Extraction of ChloA and NicoA Using the ATPSs {Ethyl Lactate (1) + NaKTartrate or Na_3Citrate or K_3Citrate (2) + Water (3)} at T = 298.15 K and P = 0.1 MPa[a]

tie-line	phase	m/ g	L_m / %	ρ / kg·m^{-3}	pH
ChloA in {Ethyl Lactate (1) + NaKTartrate (2) + Water (3)}					
1	top	4.0797	−0.33	1055.39	7.36
	bottom	5.8800		1149.51	7.67
2	top	4.4622	−0.23	1051.22	7.30
	bottom		5.5050	1167.06	7.66
3	top	4.7643	−0.31	1048.62	7.21
	bottom		5.1800	1185.88	7.81
4	top	5.1133	−0.24	1047.80	7.38
	bottom	4.8300		1201.40	7.82
5	top	5.2579	−0.27	1043.40	7.59
	bottom	4.7100		1221.45	7.78
NicoA in {Ethyl Lactate (1) + NaKTartrate (2) + Water (3)}					
1	top	4.0240	−0.64	1057.27	7.39
	bottom	5.9400		1152.70	7.80
2	top	4.5047	−0.41	1054.90	7.40
	bottom	5.4500		1166.90	7.80
3	top	4.7141	−0.53	1050.10	7.44
	bottom	5.2500		1185.30	8.40
4	top	5.1166	−0.62	1049.20	7.45
	bottom	4.8100		1201.50	7.50
5	top	5.5049	−0.74	1047.00	7.56
	bottom	4.4100		1225.00	8.10
ChloA in {Ethyl Lactate (1) + Na_3Citrate (2) + Water (3)}					
1	top	3.6872	−0.29	1052.48	7.68
	bottom	6.2700		1127.29	7.75
2	top	3.9634	−0.21	1048.21	7.66
	bottom	6.0000		1140.20	7.92
3	top	4.4286	−0.52	1046.38	7.70
	bottom	5.5600		1158.07	7.90
4	top	4.7013	−0.30	1044.83	7.75
	bottom	5.2800		1173.38	8.00
5	top	4.9230	−0.32	1043.05	7.71
	bottom	5.0700		1187.65	7.94
6	top	5.1453	−0.23	1042.43	7.73
	bottom	4.8200		1201.17	7.80
ChloA in {Ethyl Lactate (1) + K_3Citrate (2) + Water (3)}					
1	top	4.3574	−0.58	1058.89	7.96
	bottom	5.6350		1152.43	8.05
2	top	4.7951	−0.26	1054.04	7.93
	bottom	5.1900		1169.12	8.40
3	top	4.9532	−0.27	1048.43	7.90
	bottom	5.0100		1187.74	8.10
4	top	5.1455	−0.36	1045.13	7.95
	bottom	4.8400		1203.19	8.10
5	top	5.2563	−0.48	1045.51	7.94
	bottom	4.7200		1221.88	8.15
6	top	5.4748	−0.16	1045.49	8.05
	bottom	4.5050		1236.83	8.20
NicoA in {Ethyl Lactate (1) + K_3Citrate (2) + Water (3)}					
1	top	4.5855	−0.40	1062.49	7.95
	bottom	5.4000		1152.52	8.70
2	top	4.8293	−0.84	1054.93	7.98
	bottom	5.1000		1170.21	8.40
3	top	4.8026	−0.75	1051.66	8.00
	bottom	5.1000		1186.15	8.80
4	top	5.0604	−0.53	1049.57	8.04
	bottom	4.8500		1205.13	9.80
5	top	5.4146	−0.56	1046.58	8.04
	bottom	4.4800		1222.39	9.00
6	top	5.3281	−0.61	1044.63	8.03
	bottom	4.6000		1239.19	8.90

[a]The standard measurement uncertainties (u) are $u(m) = 10^{-4}$ g, $u(\rho)$ = 0.03 kg m^{-3}, u(pH) = 10^{-2}, $u(T)$ = 0.01 K, and $u(P)$ = 2 kPa.

Therefore, there must exist a significant difference in the polarity of the two molecules in addition to the similar mean electrical charges. This may happen due to the minimization of dipole moments by changes in chemical conformation, which can be investigated using computational chemistry.

More precisely, the nonrandomness factor (α) of a chemical species translates how the dipole moments are canceled out, theoretically ranging from 0 (completely random state) to 1 (completely defined spatial orientation), for which larger values of this parameter imply higher polarity (e.g., 0.3333 for water and 0.1194 for ethyl lactate).[31] Hence, DFT was applied to calculate the nonrandomness factors (α) of the species of each antioxidant (*i.e.*,ChloA^{-1} and NicoA^{-1} at pH = 7), following a previous work of the research group.[31] Specifically, the Gaussian G09 R-D.01 software[32] was used, combining the hybrid functional B3LYP[33,34] with the basis set 6-311++G(d)[35] and simulating a solvent cavity with the polarizable continuum model (PCM).[36−38] Some required properties of the studied solvents (water and ethyl lactate) for DFT calculations are shown in Table S3 in the Supporting Information.[39−43]

Following this methodology, the nonrandomness factors (α) of the antioxidant species were determined as 0.10321 in water and 0.08738 in ethyl lactate for chlorogenate (ChloA^{-1}) and 0.2861 in water and 0.1924 in ethyl lactate for nicotinate (NicoA^{-1}), for which the latter antioxidant is more polar. For this reason, the bottom phases (which are more polar) are better at solubilizing NicoA, causing solute migration toward this phase and yielding lower partition coefficients. Therefore, DFT can become very useful in providing a rough estimate for the migration of biomolecules in the phases of an ATPS, allowing one to distinguish between species with similar mean electrical charges.

Regarding the extraction efficiencies, as Figure 5 illustrates, a similar behavior was noticed with the length of tie-line (TLL), with ChloA generally respecting the order Na_3Citrate > NaKTartrate > K_3Citrate and NicoA following the opposite one. Once again, longer tie-lines favored upward solute migration, with extraction efficiencies (or mass recoveries) achieving about 90% for both antioxidants, which constitute very good results.

Nevertheless, from an industrial perspective, not only the recovery of antioxidant must be significant but also that of the solvents must not undermine the eco-friendly character of the extractions. Therefore, a process for the purification of antioxidants from biowaste using ATPSs based on ethyl lactate is suggested in Figure 6, in which the solvents are recovered by vacuum distillation. Moreover, the studied organic salts are widely used as food preservatives and pH stabilizers,[44] for which

https://doi.org/10.1021/acs.jced.4c00197
J. Chem. Eng. Data 2024, 69, 3075−3084

Table 5. Tie-Line Length (TLL), Antioxidant Mass Fraction ($w_{antioxidant}$), Partition Coefficient (K), Solute Loss in Quantification (L_s), and Extraction Efficiency (E) for Each Tie-Line Composition in the Extraction of ChloA and NicoA Using the ATPSs {Ethyl Lactate (1) + NaKTartrate or Na_3Citrate or K_3Citrate (2) + Water (3)}, at T = 298.15 K and P = 0.1 MPa[a]

tie-line	TLL / %	phase	$w_{antioxidant}$	K	L_s / %	E/ %
		ChloA in {Ethyl Lactate (1) + NaKTartrate (2) + Water (3)}				
1	43.10	top	7.35×10^{-5}	3.5 ± 0.2	−1.30	71.7 ± 0.6
		bottom	1.92×10^{-5}			
2	52.13	top	7.46×10^{-5}	4.5 ± 0.2	−1.94	78.7 ± 0.7
		bottom	1.49×10^{-5}			
3	60.15	top	7.46×10^{-5}	5.8 ± 0.4	−1.34	84.6 ± 0.8
		bottom	1.14×10^{-5}			
4	64.59	top	7.13×10^{-5}	7.4 ± 0.6	−2.85	87.4 ± 0.8
		bottom	8.40×10^{-6}			
5	70.73	top	7.15×10^{-5}	8.0 ± 0.7	−2.74	88.8 ± 0.8
		bottom	7.60×10^{-6}			
		NicoA in {Ethyl Lactate (1) + NaKTartrate (2) + Water (3)}				
1	43.10	top	3.39×10^{-4}	2.39 ± 0.07	−0.93	63.3 ± 0.4
		bottom	1.30×10^{-4}			
2	52.13	top	3.43×10^{-4}	2.9 ± 0.1	−1.08	72.0 ± 0.6
		bottom	1.06×10^{-4}			
3	60.15	top	3.40×10^{-4}	3.2 ± 0.2	−2.56	74.7 ± 0.6
		bottom	9.31×10^{-5}			
4	64.59	top	3.31×10^{-4}	3.7 ± 0.2	−3.04	79.5 ± 0.7
		bottom	7.73×10^{-5}			
5	70.73	top	3.28×10^{-4}	4.7 ± 0.3	−2.33	85.3 ± 0.8
		bottom	5.94×10^{-5}			
		ChloA in {Ethyl Lactate (1) + Na_3Citrate (2) + Water (3)}				
1	37.85	top	7.17×10^{-5}	3.1 ± 0.1	−1.05	65.3 ± 0.5
		bottom	2.17×10^{-5}			
2	48.18	top	7.58×10^{-5}	4.1 ± 0.2	−2.22	73.0 ± 0.6
		bottom	1.70×10^{-5}			
3	55.17	top	7.52×10^{-5}	5.4 ± 0.3	−2.44	80.7 ± 0.7
		bottom	1.26×10^{-5}			
4	61.17	top	7.44×10^{-5}	6.5 ± 0.4	−2.15	84.8 ± 0.8
		bottom	1.02×10^{-5}			
5	65.44	top	7.48×10^{-5}	8.8 ± 0.8	−1.27	89.6 ± 0.9
		bottom	7.44×10^{-6}			
6	69.68	top	7.23×10^{-5}	10 ± 1	−2.43	90.4 ± 0.9
		bottom	6.17×10^{-6}			
		ChloA in {Ethyl Lactate (1) + K_3Citrate (2) + Water (3)}				
1	45.91	top	6.85×10^{-5}	3.5 ± 0.2	−3.20	72.1 ± 0.6
		bottom	1.80×10^{-5}			
2	54.02	top	6.75×10^{-5}	4.2 ± 0.2	−3.13	78.4 ± 0.6
		bottom	1.45×10^{-5}			
3	62.96	top	6.97×10^{-5}	5.5 ± 0.4	−2.89	83.4 ± 0.7
		bottom	1.11×10^{-5}			
4	68.28	top	6.96×10^{-5}	6.7 ± 0.5	−2.69	86.6 ± 0.8
		bottom	8.99×10^{-6}			
5	73.92	top	6.94×10^{-5}	7.9 ± 0.7	−3.48	87.7 ± 0.8
		bottom	7.53×10^{-6}			
6	77.66	top	6.82×10^{-5}	9 ± 1	−2.60	90.5 ± 0.8
		bottom	6.10×10^{-6}			
		NicoA in {Ethyl Lactate (1) + K_3Citrate (2) + Water (3)}				
1	45.91	top	3.39×10^{-4}	2.9 ± 0.1	−1.15	69.8 ± 0.5
		bottom	3.47×10^{-4}			
2	54.02	top	3.58×10^{-4}	3.5 ± 0.2	−1.66	75.1 ± 0.6
		bottom	3.17×10^{-4}			
3	62.96	top	3.54×10^{-4}	4.3 ± 0.2	−1.53	78.6 ± 0.7
		bottom	3.00×10^{-4}			
4	68.28	top	3.69×10^{-4}	5.0 ± 0.3	−2.09	81.5 ± 0.7
		bottom	2.67×10^{-4}			
5	73.92	top	3.90×10^{-4}	5.9 ± 0.4	−2.22	84.8 ± 0.8
		bottom	2.30×10^{-4}			

https://doi.org/10.1021/acs.jced.4c00197
J. Chem. Eng. Data 2024, 69, 3075−3084

Table 5. continued

tie-line	TLL / %	phase	$w_{antioxidant}$	K	L_s / %	E/ %
		NicoA in {Ethyl Lactate (1) + K_3Citrate (2) + Water (3)}				
6	77.66	top	3.83×10^{-4}	6.5 ± 0.5	−0.73	86.8 ± 0.8
		bottom	2.29×10^{-4}			

[a]The standard measurement uncertainties (u) are $u(T)$ = 0.01 K and $u(P)$ = 2 kPa.

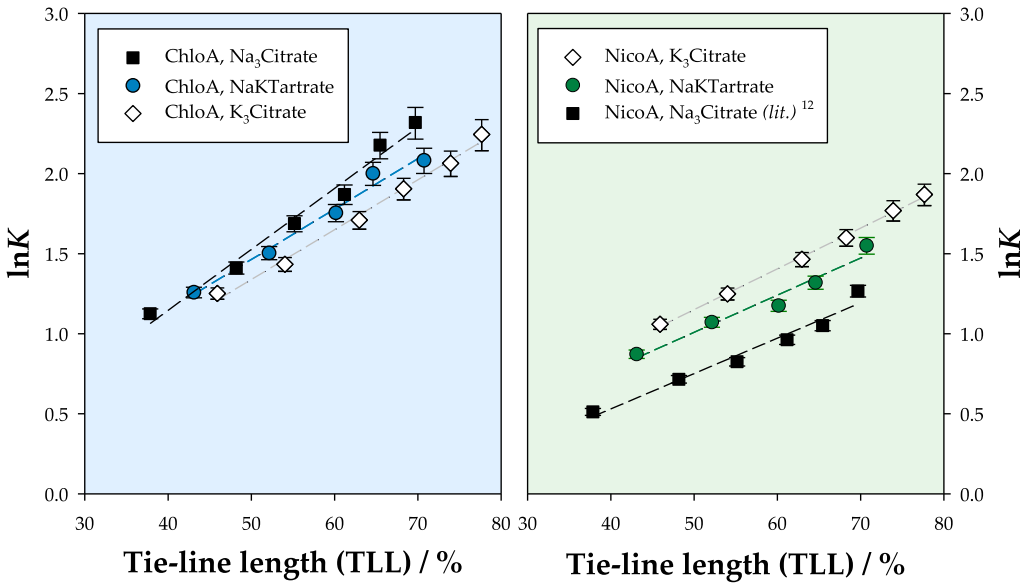

Figure 4. Natural logarithm of the partition coefficients (K) with TLL for the extraction of ChloA and NicoA in the ATPSs {ethyl lactate (1) + NaKTartrate or Na_3Citrate or K_3Citrate (2) + water (3)} at 298.15 K and 0.1 MPa. Data for NicoA in the ATPS composed of Na_3Citrate were reported in a previous work of the research group.[12]

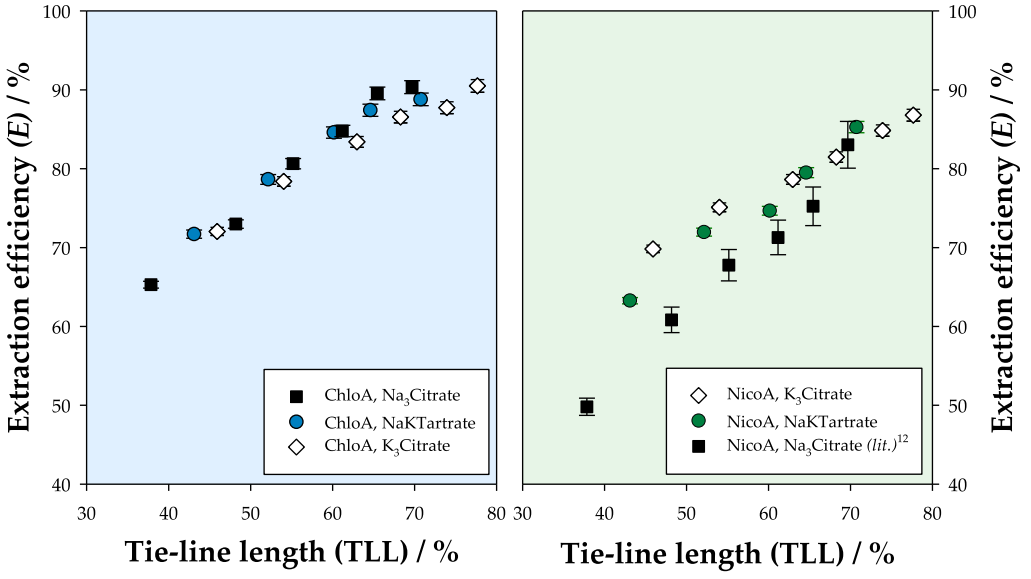

Figure 5. Extraction efficiencies (E) with TLL for the extraction of ChloA and NicoA in the ATPSs {ethyl lactate (1) + NaKTartrate or Na_3Citrate or K_3Citrate (2) + water (3)} at 298.15 K and 0.1 MPa. Data for NicoA in the ATPS composed of Na_3Citrate were reported in a previous work of the research group.[12]

their residues can be kept in the final product by joint microencapsulation (*e.g.*, food supplements and cosmetics).

4. CONCLUSIONS

In this work, the liquid−liquid extractions of ChloA and NicoA were performed in the ATPSs {ethyl lactate (1) + NaKTartrate or Na_3Citrate or K_3Citrate (2) + water (3)} at 298.15 K and 0.1 MPa. The most promising performance indicators for ChloA were obtained using Na_3Citrate, achieving a partition coefficient (K) of 10 ± 1 and an extraction efficiency (E) of 90.4 ± 0.9% in the longest tie-line (TLL = 69.68%), while for NicoA, the most successful extraction, with K = 6.5 ± 0.5 and E = 86.8 ± 0.8%, was observed in the longest tie-line (TLL = 77.66%) of the ATPS with K_3Citrate.

https://doi.org/10.1021/acs.jced.4c00197
J. Chem. Eng. Data 2024, 69, 3075−3084

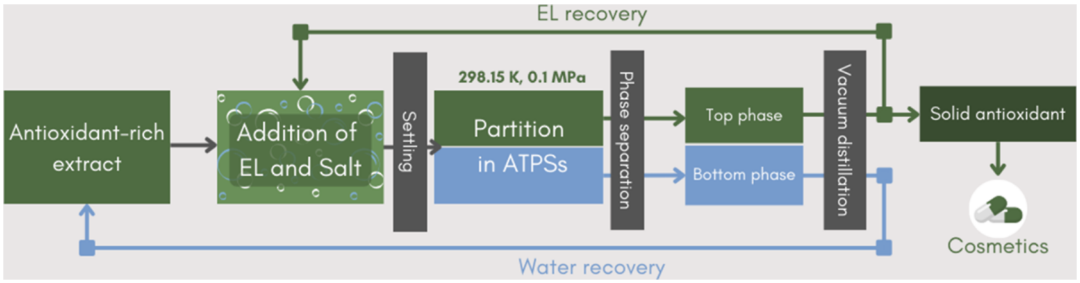

Figure 6. Suggested process for the recovery of antioxidants from food waste using ATPSs.

The obtained partition coefficients and extraction efficiencies were checked by calculating the mass losses in quantification (L_s), which were lower than 4%, validating the analytical method and allowing to conclude that the studied ATPSs based on ethyl lactate could provide an efficient and eco-friendly extraction medium for NicoA and ChloA. Moreover, computational chemistry (DFT) was used to calculate the nonrandomness factors (α) of the present species of each antioxidant and to validate the top-phase-oriented solute migration.

■ ASSOCIATED CONTENT

Supporting Information

The Supporting Information is available free of charge at https://pubs.acs.org/doi/10.1021/acs.jced.4c00197.

Chemical structures and mean electrical charges (q) of the studied antioxidants; phase diagrams of the used ATPSs; calculated partition coefficients (K) based on concentrations in different units; and thermophysical properties of the solvents used in computational chemistry (PDF)

■ AUTHOR INFORMATION

Corresponding Authors

Pedro Velho − *LSRE-LCM−Laboratory of Separation and Reaction Engineering—Laboratory of Catalysis and Materials, Faculty of Engineering, University of Porto, Porto 4200-465, Portugal; ALiCE—Associate Laboratory in Chemical Engineering, Faculty of Engineering, University of Porto, Porto 4200-465, Portugal;* orcid.org/0000-0003-4802-7301; Email: velho@fe.up.pt

Gonçalo Perestrelo − *LSRE-LCM−Laboratory of Separation and Reaction Engineering—Laboratory of Catalysis and Materials, Faculty of Engineering, University of Porto, Porto 4200-465, Portugal; ALiCE—Associate Laboratory in Chemical Engineering, Faculty of Engineering, University of Porto, Porto 4200-465, Portugal*; Email: up201908045@edu.fe.up.pt

Eugénia A. Macedo − *LSRE-LCM−Laboratory of Separation and Reaction Engineering—Laboratory of Catalysis and Materials, Faculty of Engineering, University of Porto, Porto 4200-465, Portugal; ALiCE—Associate Laboratory in Chemical Engineering, Faculty of Engineering, University of Porto, Porto 4200-465, Portugal;* orcid.org/0000-0002-0724-5380; Email: eamacedo@fe.up.pt

Complete contact information is available at: https://pubs.acs.org/10.1021/acs.jced.4c00197

Notes

The authors declare no competing financial interest.

■ ACKNOWLEDGMENTS

This work was supported by national funds through FCT/MCTES (PIDDAC): LSRE-LCM, UIDB/50020/2020 (DOI: 10.54499/UIDB/50020/2020), UIDP/50020/2020 (DOI: 10.54499/UIDP/50020/2020), and ALiCE, LA/P/0045/2020 (DOI: 10.54499/LA/P/0045/2020). P.V. is grateful for the funding support from FCT [2021.06626.BD].

■ REFERENCES

(1) Kibler, K. M.; Reinhart, D.; Hawkins, C.; Motlagh, A. M.; Wright, J. Food waste and the food-energy-water nexus: A review of food waste management alternatives. *Waste Manage.* **2018**, *74*, 52−62.

(2) Ma, K.; Li, F.; Zhe, T.; Sun, X.; Zhang, X.; Wan, P.; Na, H.; Zhao, J.; Wang, L. Biopolymer films incorporated with chlorogenic acid nanoparticles for active food packaging application. *Food Chem.* **2024**, *435*, 137552.

(3) Chao, M.; Ma, X. Voltammetric determination of chlorogenic acid in pharmaceutical products using poly(aminosulfonic acid) modified glassy carbon electrode. *J. Food Drug Anal.* **2014**, *22*, 512−519.

(4) Santana-Gálvez, J.; Cisneros-Zevallos, L.; Jacobo-Velázquez, D. Chlorogenic Acid: Recent Advances on Its Dual Role as a Food Additive and a Nutraceutical against Metabolic Syndrome. *Molecules* **2017**, *22*, 358.

(5) Bodor, E. T.; Offermanns, S. Nicotinic acid: An old drug with a promising future. *Br. J. Pharmacol.* **2008**, *153*, S68−S75.

(6) Gonçalves, B.; Moeenfard, M.; Rocha, F.; Alves, A.; Estevinho, B. N.; Santos, L. Microencapsulation of a Natural Antioxidant from Coffee—Chlorogenic Acid (3-Caffeoylquinic Acid). *Food Bioprocess Technol.* **2017**, *10*, 1521−1530.

(7) Çat, J.; Yaman, M. Determination of Nicotinic Acid and Nicotinamide Forms of Vitamin B3 (Niacin) in Fruits and Vegetables by HPLC Using Postcolumn Derivatization System. *Pak. J. Nutr.* **2019**, *18*, 563−570.

(8) Torres-Acosta, M. A.; dos Santos, N. V.; Ventura, S. P. M.; Coutinho, J. A. P.; Rito-Palomares, M.; Pereira, J. F. B. Economic analysis of the production and recovery of green fluorescent protein using ATPS-based bioprocesses. *Sep. Purif. Technol.* **2021**, *254*, 117595.

(9) Gu, Z.; Glatz, C. E. Aqueous two-phase extraction for protein recovery from corn extracts. *J. Chromatogr. B* **2007**, *845*, 38−50.

(10) Wang, L.; Wang, Y.; Qin, Y.; Liu, B.; Zhou, Y. Extraction and Determination of Protein from Edible Oil Using Aqueous Biphasic Systems of Ionic Liquids and Salts. *Food Bioprocess Technol.* **2022**, *15*, 190−202.

(11) Li, Y.; Lu, X.; Zhu, Q.; Huang, R.; Hu, J.; Yang, H.; Yao, Y. Phase behavior of quaternary aqueous two-phase systems: Influence factors and extraction mechanism study. *Fluid Phase Equilib.* **2016**, *430*, 101−111.

(12) Velho, P.; Marques, L.; Macedo, E. A. Extraction of Polyphenols and Vitamins Using Biodegradable ATPS Based on Ethyl Lactate. *Molecules* **2022**, *27*, 7838.

(13) Chakraborty, A.; Mukhopadhyay, C.; Sen, K. Block copolymer and organic salts in forming aqueous biphases: a platform to identify molecular interactions in aqueous medium†. *RSC Adv.* **2016**, *6*, 77673−77681.

(14) Teymoornejad, G.; Jabbari, M. Bioactive flavonoids partitioning in a deep eutectic solvent/surfactant aqueous biphasic system: Efficiency and thermodynamics. *Colloids Surf., A* **2024**, *687*, 133541.
(15) Rebelo, C. S.; Velho, P.; Macedo, E. A. Partition Studies of Resveratrol in Low-Impact ATPS for Food Supplementation. *Ind. Eng. Chem. Res.* **2024**, *63*, 2885−2894.
(16) Li, R.; Kang, K.; Li, J.; Wang, S.; Hang, F. Sustainable aqueous biphasic system created using sugar-based deep eutectic solvents/ethyl lactate for the green extraction of biomolecules. *J. Mol. Liq.* **2024**, *399*, 124474.
(17) Das, L.; Sen, K. Carbohydrate-Tailored PPG#400 vs Ionic Liquid-Based Aqueous Biphasic System That Enables Extraction of Polyphenols. *J. Chem. Eng. Data* **2023**, *68*, 2398−2406.
(18) Madadi, B.; Pazuki, G.; Nasernejad, B. Partitioning of Cefazolin in Biocompatible Aqueous Biphasic Systems Based on Surfactant. *J. Chem. Eng. Data* **2013**, *58*, 2785−2792.
(19) Velho, P.; Barroca, L. R.; Macedo, E. A. Partition of antioxidants available in biowaste using a green aqueous biphasic system. *Sep. Purif. Technol.* **2023**, *307*, 122707.
(20) Karthika, S.; Radhakrishnan, T. K.; Kalaichelvi, P. Crystallization and Kinetic Studies of an Active Pharmaceutical Compound Using Ethyl Lactate As a Green Solvent. *ACS Sustainable Chem. Eng.* **2020**, *8*, 1527−1537.
(21) Dai, S.-B.; Lee, H.-Y.; Chen, C.-L. Design and Economic Evaluation for the Production of Ethyl Lactate via Reactive Distillation Combined with Various Separation Configurations. *Ind. Eng. Chem. Res.* **2019**, *58*, 6121−6132.
(22) Burke, K. Perspective on density functional theory. *J. Chem. Phys.* **2012**, *136*, 150901.
(23) Marrazzini, G.; Giovannini, T.; Scavino, M.; Egidi, F.; Cappelli, C.; Koch, H. Multilevel Density Functional Theory. *J. Chem. Theory Comput.* **2021**, *17*, 791−803.
(24) Requejo, P. F.; Velho, P.; Gómez, E.; Macedo, E. A. Study of Liquid-Liquid Equilibrium of Aqueous Two-Phase Systems Based on Ethyl Lactate and Partitioning of Rutin and Quercetin. *Ind. Eng. Chem. Res.* **2020**, *59*, 21196−21204.
(25) Velho, P.; Requejo, P. F.; Gómez, E.; Macedo, E. A. Novel ethyl lactate based ATPS for the purification of rutin and quercetin. *Sep. Purif. Technol.* **2020**, *252*, 117447.
(26) Wysoczanska, K.; Nierhauve, B.; Sadowski, G.; Macedo, E. A.; Held, C. Solubility of DNP-amino acids and their partitioning in biodegradable ATPS: Experimental and ePC-SAFT modeling. *Fluid Phase Equilib.* **2021**, *527*, 112830.
(27) Wysoczanska, K.; Do, H. T.; Sadowski, G.; Macedo, E. A.; Held, C. Partitioning of water-soluble vitamins in biodegradable aqueous two-phase systems: Electrolyte perturbed-chain statistical associating fluid theory predictions and experimental validation. *AIChE J.* **2020**, *66*, No. e16984.
(28) Maegawa, Y.; Sugino, K.; Sakurai, H. Identification of free radical species derived from caffeic acid and related polyphenols. *Free Radical Res.* **2007**, *41*, 110−119.
(29) Hughes, E. B.; Jellinek, H. H. G.; Ambrose, B. A. Nicotinic Acid. Ultraviolet Absorption Spectrum and Dissociation Constants. *J. Phys. Chem.* **1949**, *53*, 414−423.
(30) Velho, P.; Macedo, E. A. Liquid-Liquid Extraction of Some Biomolecules in the ATPS {Ethyl Lactate (1) + Sodium Potassium Tartrate (2) + Water (3)} at 298.15 K and 0.1 MPa. *J. Chem. Eng. Data* **2023**, *68*, 2385−2397.
(31) Velho, P.; Barroca, L. R.; Macedo, E. A. A Geometric Approach for the Calculation of the Nonrandomness Factor Using Computational Chemistry. *J. Chem. Eng. Data* **2024**, DOI: 10.1021/acs.jced.3c00532.
(32) Frisch, M. J.; Trucks, G. W.; Schlegel, H. B.; Scuseria, G. E.; Robb, M. A.; Cheeseman, J. R.; Scalmani, G.; Barone, V.; Mennucci, B.; Petersson, G. A.; et al. *Guassian 09*: Revision D.01; Guassian, 2009.
(33) Becke, A. D. Density-functional thermochemistry. III. The role of exact exchange. *J. Chem. Phys.* **1993**, *98*, 5648−5652.
(34) Lee, C.; Yang, W.; Parr, R. G. Development of the Colle-Salvetti correlation-energy formula into a functional of the electron density. *Phys. Rev. B: Condens. Matter Mater. Phys.* **1988**, *37*, 785−789.
(35) Francl, M. M.; Pietro, W. J.; Hehre, W. J.; Binkley, J. S.; Gordon, M. S.; DeFrees, D. J.; Pople, J. A. Self-consistent molecular orbital methods. XXIII. A polarization-type basis set for second-row elements. *J. Chem. Phys.* **1982**, *77*, 3654−3665.
(36) Miertuš, S.; Scrocco, E.; Tomasi, J. Electrostatic interaction of a solute with a continuum. A direct utilizaion of AB initio molecular potentials for the prevision of solvent effects. *Chem. Phys.* **1981**, *55*, 117−129.
(37) Miertuš, S.; Tomasi, J. Approximate evaluations of the electrostatic free energy and internal energy changes in solution processes. *Chem. Phys.* **1982**, *65*, 239−245.
(38) Pascual-ahuir, J. L.; Silla, E.; Tuñon, I. GEPOL: An improved description of molecular surfaces. III. A new algorithm for the computation of a solvent-excluding surface. *J. Comput. Chem.* **1994**, *15*, 1127−1138.
(39) Aparicio, S.; Halajian, S.; Alcalde, R.; García, B.; Leal, J. M. Liquid structure of ethyl lactate, pure and water mixed, as seen by dielectric spectroscopy, solvatochromic and thermophysical studies. *Chem. Phys. Lett.* **2008**, *454*, 49−55.
(40) Cepeda, E. A.; Urbano, C. Isobaric Vapor Liquid Equilibrium of 3-Methyl-1-butanol + Ethyl Lactate and 1-Pentanol + Ethyl Lactate at (13.0 and 101.3) kPa. *J. Chem. Eng. Data* **2011**, *56*, 2602−2607.
(41) Owen, B. B.; Miller, R. C.; Milner, C. E.; Cogan, H. L. The dielectric constant of water as a function of temperature and pressure. *J. Phys. Chem.* **1961**, *65*, 2065−2070.
(42) Hale, G. M.; Querry, M. R. Optical Constants of Water in the 200-nm to 200-μm Wavelength Region. *Appl. Opt.* **1973**, *12*, 555−563.
(43) Tanaka, M.; Girard, G.; Davis, R.; Peuto, A.; Bignell, N. Recommended table for the density of water between 0 °C and 40 °C based on recent experimental reports. *Metrologia* **2001**, *38*, 301−309.
(44) Rebelo, C. S.; Velho, P.; Macedo, E. A. eNRTL Modelling and Partition of Phenolics in the ATPSs {Ethyl lactate (1) + Potassium Sodium Tartrate or Disodium Succinate (2) + Water (3)} at 298.2 K and 0.1 MPa. *Fluid Phase Equilib.* **2024**, *582*, 114087.